

# Photonic lanterns: a study of light propagation in multimode to single-mode converters

Sergio G. Leon-Saval\*, Alexander Argyros and Joss Bland-Hawthorn

*Institute of Photonics and Optical Science, School of Physics, The University of Sydney, Australia*

*\*S.G.Leon-Saval@usyd.edu.au*

**Abstract:** The “photonic lantern,” an optical fibre device that has emerged from the field of astrophotonics, allows for a single-mode photonic function to take place within a multimode fibre. We study and evaluate the modal behaviour of photonic lanterns as well as the conditions for achieving low-loss between a multimode fibre and a “near-diffraction limited” single-mode system. We also present an intuitive analogy of the modal electromagnetic propagation behaviour along the photonic lantern transition in terms of the Kronig-Penney model in Quantum Mechanics.

©2010 Optical Society of America

**OCIS codes:** (060.2340) Fiber optics components; (350.1260) Astronomical optics.

---

## References and links

1. A. J. Horton, and J. Bland-Hawthorn, “Coupling light into few-mode optical fibres I: The diffraction limit,” *Opt. Express* **15**(4), 1443–1453 (2007).
2. J. C. Corbett, “Sampling of the telescope image plane using single- and few-mode fibre arrays,” *Opt. Express* **17**(3), 1885–1901 (2009).
3. J. Bland-Hawthorn, and P. Kern, “Astrophotonics: a new era for astronomical instruments,” *Opt. Express* **17**(3), 1880–1884 (2009).
4. D. Noordegraaf, P. M. W. Skovgaard, M. D. Nielsen, and J. Bland-Hawthorn, “Efficient multi-mode to single-mode coupling in a photonic lantern,” *Opt. Express* **17**(3), 1988–1994 (2009).
5. S. G. Leon-Saval, T. A. Birks, J. Bland-Hawthorn, and M. Englund, “Multimode fiber devices with single-mode performance,” *Opt. Lett.* **30**(19), 2545–2547 (2005).
6. F. Ladouceur, and J. Love, “Multiport single-mode fibre splitters,” *Opt. Quantum Electron.* **22**(5), 453–465 (1990).
7. S. G. Leon-Saval, T. A. Birks, N. Y. Joly, A. K. George, W. J. Wadsworth, G. Kakarantzas, and P. St. J. Russell, “Splice-free interfacing of photonic crystal fibers,” *Opt. Lett.* **30**(13), 1629–1631 (2005).
8. A system of  $m$  single-mode cores will in fact support  $2m$  vector modes, corresponding to  $m$  modes each for two orthogonal polarisations. Similarly, a system of  $m$  quantum wells will support  $2m$  electron states, corresponding to  $m$  states each for two values of the electron spin. This additional complexity does not change the analogy in any way, thus it is omitted from the text to simplify the analogy.
9. T. P. White, B. T. Kuhlmeier, R. C. McPhedran, D. Maystre, G. Renversez, C. M. de Sterke, and L. C. Botten, “Multipole method for microstructured optical fibres I: Formulation,” *J. Opt. Soc. Am. B* **19**(10), 2322–2330 (2002).
10. <http://www.physics.usyd.edu.au/cudos/mofsoftware/>.
11. N. A. Issa, and L. Poladian, “Vector wave expansion method for leaky modes of microstructured optical fibers,” *J. Lightwave Technol.* **21**(4), 1005–1012 (2003).
12. <http://code.google.com/p/polymode/>.
13. W. Snyder, and J. D. Love, *Optical Waveguide Theory* (Chapman & Hall, 1983).
14. R. J. Black, J. Lapiere, and J. Bures, “Field evolution in doubly clad lightguides,” *IEE Proc.-J: Optoelectron.* **134**, 105 (1987).
15. Although the lowest order core mode would ordinarily not go below the cladding index (1.444 here), it does in this case due to the finite cladding, and the presence of the lower index outer cladding.

---

## 1. Introduction

Multimode fibres are widely used in optical and infrared astronomy to allow many celestial sources to be observed simultaneously. These large-core fibres (50–300 $\mu\text{m}$  core diameter) are used to transport light from the telescope focal plane to a remote spectrograph. Mainstream astronomy has tended to avoid single-mode fibres because of the difficulty of coupling light into these efficiently. Even the best performing adaptive optics systems, which attempt to

deliver a diffraction-limited beam, are unable to couple light efficiently into the Gaussian beam of single-mode fibres below 2500 nm [1,2]. Consequently, astronomers have been unable to exploit numerous technological advances in photonics over the past three decades.

Astro-photonics, a field that lies at the interface of astronomy and photonics, has emerged over the past decade to explore the wider application of photonics in astronomical and space instrumentation [3]. One of the first technologies to emerge was the remarkable photonic lantern [4,5]. This is an optical fibre device that couples light from a multimode fibre (MMF) to single-mode fibres (SMFs) or single-mode cores, and vice versa. The capability of coupling light from a multimode fibre to a single-mode system in which the light is propagating in several Gaussian modes (i.e. modes that can be focused to the diffraction limit) is remarkable. As such, for this work we will consider the single-mode propagation in the optical fibres to be “near-diffraction limited”. The lantern comprises an array of isolated identical SMF cores as a degenerate multimode system, in which the near-diffraction limited spatial modes are the supermodes of the array. The number of degenerate supermodes is equal to the number of cores, and their propagation constants equal that of the mode of a single core in isolation [6]. Light can couple between the array of SMFs and a MMF via a gradual taper transition. If the transition is adiabatic, then the supermodes of the SMF array evolve into the modes of the MMF core, and vice versa. The second law of thermodynamics (brightness theorem) does not allow lossless coupling of light from an arbitrarily excited MMF into one SMF, but if the effectively multimode system to be coupled to (i.e SMF array) has the same number of degrees of freedom, then lossless coupling becomes possible. Hence, a low-loss adiabatic

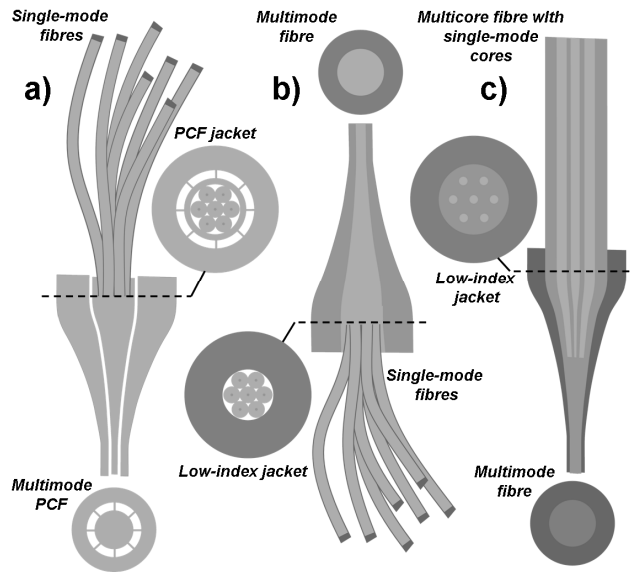


Fig. 1. Schematic representation of the three different approaches for the fabrication of Photonic lanterns; a) PCF technique; b) Standard single-mode fibre combiner/splitter technique; and c) Multicore fibre approach.

transition between a MMF with  $m$  modes and an array of  $m$  SMFs is theoretically possible. Such transitions would couple light from an array of SMFs with  $m$  degenerate supermodes to a MMF core with  $m$  modes, and vice versa.

Photonic lanterns to date have been manufactured and demonstrated by two different techniques, in both cases the single-mode cores are reduced in size so as to become ineffective waveguides, and the light at the MMF end becomes confined by a second, outer cladding as shown in Fig. 1. The first multimode transition with single-mode performance [5] was demonstrated by using a technique [7] for interfacing SMFs to photonic crystal fibres (PCFs)

as shown in Fig. 1(a). A more recent approach was demonstrated by Noordegraaf et al [4], where an all solid standard optical fibre splitter/combiner technique was used. A bundle of SMFs was inserted into a low index glass capillary tube which was then fused and tapered down to form an all solid MMF at the other end (Fig. 1(b)). As reported previously in [5], another interesting approach for the realization of these multimode to single-mode transitions is by using a multicore fibre with an array of identical single-mode cores. A photonic lantern can be made by tapering such a multicore fibre while placing a low refractive index jacket around the fibre to form the cladding of the MMF (see Fig. 1(c)). However, from those three approaches, only the first two use individual SMFs, thus they have an intrinsically near-diffraction limited operation at the SMF end of the photonic lantern transition. The multicore fibre approach is not intrinsically near-diffraction limited and the design of the multicore fibre itself has to be considered for near-diffraction limited (i.e. single-mode) operation.

In this paper we study and analyse the modal behaviour as well as the conditions for achieving a low-loss multimode to single-mode converter. A toy model analogy with Quantum Mechanics (QM) is also introduced, giving an intuitive explanation of the modal evolution along the photonic lantern transitions.

## 2. Quantum analogy of photonic lanterns

There exist fundamental differences between the properties of photons and electrons. They differ in charge, spin, mass, velocity, wavefunction representation and dispersion (energy versus wavevector relationship). At an atomic scale, electrons begin to display wavelike properties, including interference and non-localization. This information is contained within the wave-function which obeys the wave-Eq. (-)like Schrödinger equation. A free electron may be represented by a plane wave, whereas for conduction electrons inside a periodic crystal, as in the Kronig-Penney model, the electron wavefunction is described by the Bloch function. Here we will present an analogy of the electromagnetic modal propagation behaviour within a photonic lantern in terms of the single-electron 1D Kronig-Penney model in QM. We will compare a photonic transition between an isolated array of  $m$  SMFs and a MMF with  $m$  modes (i.e. the photonic lantern) to a QM system which varies from  $m$  isolated potentials, each with a single discrete allowed energy level, to a single isolated potential with  $m$  discrete energy levels [8]. Thus we compare optical fibre cores with quantum wells.

In order to make this analogy we sketch the typical one dimensional refractive index profile ( $n$ ) vs. radius widely used for optical fibres, but using  $1/n$  instead of  $n$  in the vertical axis. This simple inversion allows the refractive index profile of our photonic lantern to be represented in the same fashion as the 1D Kronig-Penney model of periodic potentials ( $V$ ) vs. length as shown in Fig. 2. In the QM case, energy is used to define the wavefunctions corresponding to discrete energy levels, however this is not applicable to the electromagnetic (EM) case of spatial modes propagating along a fibre core, as the energy of each photon is fixed ( $E = hf$ ). These spatial modes in the EM case are defined by their propagation constant  $\beta = Kn_{eff}$  ( $K$  being the wavenumber) and a transverse wavenumber  $K_T$  (see Fig. 2), modes with high  $n_{eff}$  having low  $K_T$ . In our analogy of the mode evolution,  $K_T$  (EM) and  $E$  (QM) behave qualitatively the same. We compare the change in energy of the standing wave solutions of the electron inside the quantum wells with the change in  $K_T$  of the spatial modes in the waveguide. With these in mind, at each point of the photonic lantern transition we can define a scenario for an electron wave solution in a periodic potential well which would represent a perfect analogy to the behaviour of the modal propagation and coupling of the photonic lantern supermodes.

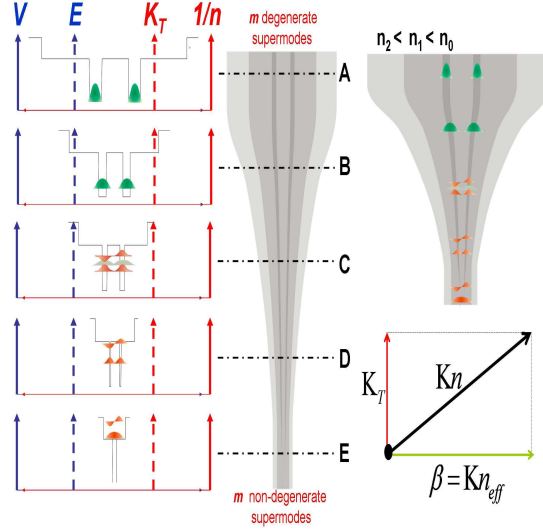


Fig. 2. A schematic evolution of supermodes throughout the tapered transition of the photonic lantern with two single-mode cores. (Left) Inverse of the refractive index profile ( $1/n$ ) vs. radius compared to the analogous QM 1D Kronig-Penney quantum well structure. For the vertical axis a comparison is made between transverse wavevectors ( $K_T$ ) of photons and energy of the electron ( $E$ ) at different positions along the tapered transition. The sketched modes' height with respect to the vertical axis represents the change in  $K_T$  and  $E$  for the EM wave case and for the QM case respectively. (Top right) Details of refractive indices within the structure of the photonic lantern. (Bottom right) Vectorial decomposition of the  $K_n$  wavevector.

For the purposes of the analogy, the propagation direction is chosen as being from the uncoupled single-mode fibres towards the multimode fibre. At the start of the transition (point A in Fig. 2), we have an  $m$  number of SMFs or uncoupled cores of a multicore fibre system. At this point the photonic lantern will support  $m$  uncoupled degenerate spatial supermodes, each being the fundamental mode of the individual SMFs or cores. With the right refractive index and geometry, a fibre core can be designed to have only one spatial mode. This mode will have the highest propagation constant and its electric field concentrated in the region of high refractive index and hence the highest  $n_{eff}$  value and the lowest  $K_T$ . In the QM case of an isolated potential well, only discrete energies for the electron wavefunction are allowed, and the electron wavefunction takes the form of standing waves. With the right potential and geometry, a potential well can be designed to allow only one discrete energy level (i.e. the ground state). These standing wave solutions of the independent quantum wells have the lowest energy ( $E$ ) and typically their amplitude is concentrated in the regions of low  $V$ , those can be considered the fundamental modes.

At the beginning of the taper transition as the cores reduce in size (point B in Fig. 2), the fundamental modes of the SMFs in the photonic lantern start to spread out of the cores showing a decrease in modal effective index ( $n_{eff}$ ) and an increase in  $K_T$ . In the QMs case, as the width of the quantum wells becomes smaller, the amplitude of the standing wave solutions will be less concentrated in the region of low  $V$  showing an increase in  $E$ . As the taper transition evolves (point C in Fig. 2) the fundamental modes of each of the SMF cores become less confined and starts coupling to neighbouring cores. The well defined  $n_{eff}$  of the individual core modes (i.e.  $m$  degenerate supermodes of the array) will start splitting into a set of  $m$  non-degenerate supermodes of the composite waveguide with lower and higher  $n_{eff}$ . This  $n_{eff}$  splitting and the spatial distribution of the modes will be governed by the confinement strength of the cores. In the QM equivalent as the potential wells become narrower the ability of electrons to tunnel between barrier (potential) walls spreads out the discrete energy level seen for isolated wells into non-degenerate energy levels of higher and lower energy.

As the individual cores become gradually less significant in guidance (point D in Fig. 2), the splitting in  $n_{eff}$  of the  $m$  non-degenerate supermodes becomes more pronounced and their confinement and spatial profiles begin to be governed by the outer lower index cladding enclosing the SMF array. In the same fashion we can imagine for our analogy that our 1-D array of quantum wells is enclosed within a higher potential quantum well. This will determine the allowed values of the electron standing wave solutions in our system once the original wells become too narrow to alone influence the electronic states. At the point where the taper ends (point E in Fig. 2), the waveguide is essentially a MMF, which geometry and refractive index profile only allows  $m$  number of non-degenerate modes. At this point in the QM model, the original wells have essentially vanished, and the behaviour of the electron is described by  $m$  energy states confined by a single broader, higher potential well.

### 3. Mode evolution of a $7 \times 1$ photonic lantern

The  $7 \times 1$  photonic lantern described in [4] was modelled in order to investigate the mode evolution along the tapered transition of the lantern quantitatively. The structure of the lantern was adapted from [4] and approximated as follows: in the thicker end of the transition the seven single-mode cores ( $n_{co} = 1.45397$ ;  $d = 6.5 \mu\text{m}$ ) at  $80 \mu\text{m}$  separation were embedded in silica ( $n = 1.4440$ ) extending to a diameter of  $224 \mu\text{m}$ , in turn surrounded by the outer cladding ( $n = 1.4431$ ) extending to an outer diameter (OD) of  $437 \mu\text{m}$ . A schematic of this structure was shown in Fig. 1(b) (not to scale). Along the transition this structure was scaled down to a final OD of  $90 \mu\text{m}$ . (In [4] the transition ends at a final OD of  $110 \mu\text{m}$ .) The wavelength of operation was taken to be  $1.55 \mu\text{m}$ .

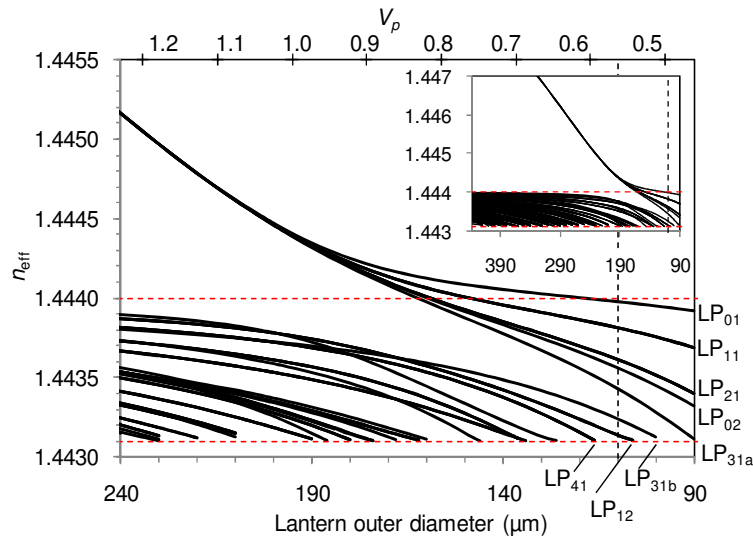


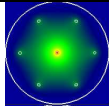
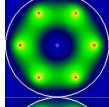
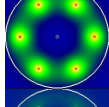
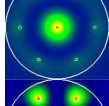
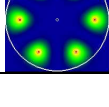
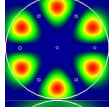
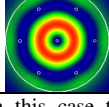
Fig. 3. The evolution of modes throughout the tapered transition of the photonic lantern. The 14 core modes are degenerate at large diameters, but become non-degenerate at smaller diameters and fill the range of  $n_{eff}$  available in the multimode core at the end of the transition. The red horizontal dashed lines indicate the core and cladding index of the final multimode core ( $n_{co} = 1.444$ ;  $n_{cl} = 1.4431$ ), and the vertical dashed line indicates the  $110 \mu\text{m}$  diameter at which the transition was terminated in [4]; more details of the modes at this point are given in Table 1. The inset shows the mode evolution over the entire transition.

The modelling was undertaken using the CUDOS MOF Utilities software [9,10] and the Polymode software [11,12]. The mode evolution along the taper transition is shown in Fig. 3 and details of the modes at an OD of  $110 \mu\text{m}$  are shown in Table 1.

At the larger OD the seven single-mode cores act as independent waveguides and the 14 vector modes supported (polarization included) by the seven cores are degenerate with an  $n_{eff}$

= 1.44885686. This independence is the result of the large separation between the cores, and the strong confinement by each core of the light guided within it, which prevent interaction between neighbouring cores. The strong confinement is reflected in the  $V_p$ - parameter, which is defined as  $V_p = \pi d/\lambda (n_{co}^2 - n_{cl}^2)^{1/2}$ , where  $d$  is the diameter of the core. At the original OD of 437  $\mu\text{m}$   $V_p = 2.2$  for each core, meaning the light is strongly confined [13]. Along the transition to smaller diameters the cores are both brought closer together and reduced in size, the latter serving to reduce  $V_p$  for the cores, meaning the light guided in each core will extend further away from it and interact more strongly with the neighbouring cores. When the OD reaches approximately 200  $\mu\text{m}$  the 14 modes of the seven cores begin to be split significantly and their separation in  $n_{eff}$  increases. This corresponds to a  $V_p \sim 1$  and such (i.e. step index) cores are known to be increasingly unable to confine light for  $V_p < 1$  [14].

**Table 1. Details of modes supported by the photonic lantern modeled in Fig. 3 at an OD of 110  $\mu\text{m}$ .**

Scalar mode	Vector modes	Degeneracy	$n_{eff}$	Near field ( $S_z$ )
LP <sub>01</sub>	HE <sub>11</sub>	2	1.44398	
LP <sub>11</sub>	HE <sub>21</sub> TE <sub>01</sub> TM <sub>01</sub>	4	1.44381	
LP <sub>21</sub>	EH <sub>11</sub> HE <sub>31</sub>	4	1.44361	
LP <sub>02</sub>	HE <sub>12</sub>	2	1.44356	
LP <sub>31a</sub> *	EH <sub>21</sub>	2	1.44343	
<b>Originally cladding modes</b>				
LP <sub>31b</sub> *	HE <sub>41</sub>	2	1.44324	
LP <sub>12</sub>	HE <sub>22</sub> TE <sub>02</sub> TM <sub>02</sub>	4	1.44314	

\*The LP<sub>31</sub> is four-fold degenerate for circularly symmetric structures. In this case the symmetry of the waveguide results in two distinct two-fold degenerate modes.

Although vector mode solutions were found in the modelling, the low index contrast in this structure warrants the use of scalar mode notation, as in Fig. 3 and Table 1. The original 14 degenerate vector modes evolve into five non-degenerate scalar modes, with each scalar mode having a two-fold or four-fold degeneracy so as to maintain 14 modes in total. The modes originating from the seven cores are distinct from the cladding modes which, at large OD, essentially form a continuum between in the range  $1.4431 < n_{eff} < 1.444$ . At smaller OD the cladding modes become cut off one by one and the original core modes evolve to take their place in the  $1.4431 < n_{eff} < 1.444$  range [15]. The two sets of modes remain clearly separated in  $n_{eff}$  throughout the whole transition. Table 1 shows a more detailed picture of the modes at 110  $\mu\text{m}$  OD. The five scalar modes originating from the cores are still somewhat

localised on the remnants of the cores. In addition, two cladding modes are still supported and these do not overlap with the core remnants.

Considering the operation of the photonic lantern, light launched at the small OD end would couple to whatever modes are supported there and evolve accordingly. Considering a final 110  $\mu\text{m}$  OD of the modelled structure (from [4]), there are seven scalar modes (20 vector modes) available as seen in Fig. 3 and Table 1, but only five of those will reach the single-mode cores at the large OD end (the other two are cladding modes). This provides an opportunity for loss, depending on the fraction of light coupled to each of the seven modes. For the modelled structure a final OD of 100  $\mu\text{m}$  may be more preferable as only the five modes corresponding to the cores are supported. Diameters  $< 90 \mu\text{m}$  will become problematic as the core modes themselves will begin to be cut off.

In the reverse case, the clear separation throughout the transition of the core and cladding modes means coupling between these modes would be negligible. Hence light launched into the core modes at the large OD end would reach the multimode fibre at the small OD end without any losses. This is an essential feature in the operation of the photonic lantern as any light coupling from the core modes to the cladding modes during the transition would be lost at the smaller OD end of the transition as the cladding modes are cut off. The presence of the additional two cladding modes at the 110  $\mu\text{m}$  OD would be of no consequence, as no light will couple to these. In this sense, the design of the photonic lantern modelled here appears to be close to optimal.

#### **4. Core geometry study: degenerate single-mode operation and modal evolution**

The operation of the photonic lantern for different single-mode core geometries will be investigated. In particular, the effects of changing the original distance between the single-mode cores at the large OD end of the transition will be examined. As previously, we consider a  $7 \times 1$  photonic lantern with all parameters identical to the previous section except for the separation between the cores.

The multicore fibre approach for the photonic lantern (Fig. 1(c)), is the only one that can in principle compromise the degenerate single-mode operation. In order to fulfil the near-diffraction limited operation, the modes of the individual cores have to be degenerate and hence uncoupled at the large OD end, whereas bringing the cores closer together at the large OD end will eventually lead to them coupling and producing non-degenerate supermodes. To investigate this, we calculated the  $n_{eff}$  at the large OD end for a range of core separations, beginning from the 80  $\mu\text{m}$  separation as modelled in the previous section and as used in [4], and then moving the cores closer together until they touch each other. (Note this is different to the photonic lantern tapered transition, as here the cores are brought closer together *without* reducing in size.) The results are shown in Fig. 4. As the cores approach each other, they begin to interact and the 14 originally degenerate vector modes produce five non-degenerate scalar supermodes, each having a two-fold or four-fold degeneracy so as to maintain 14 modes in total, as observed previously for the tapered transition.

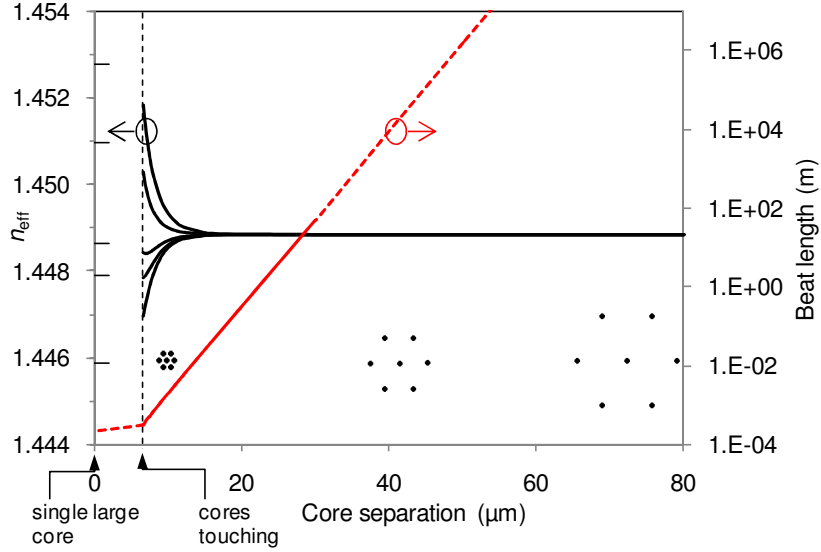


Fig. 4. Splitting of the 14 originally degenerate core modes into five non-degenerate scalar supermodes as the seven cores are brought closer together (but not reduced in size). The cores have the following properties:  $n_{co} = 1.45397$ ;  $n_{cl} = 1.444$ ;  $d = 6.5 \mu\text{m}$ . With decreasing core separation the  $n_{eff}$  of these supermodes approach those of the five modes supported by a single large multimode core with an area equal to the total area of the seven cores (i.e. with  $r_{co} = 8.6 \mu\text{m}$ ). The beat length for modal beating between the lowest and highest order modes is also indicated. A particular near field pattern will remain preserved over lengths that are short compared to this beat length.

The ‘amount’ of non-degeneracy of the modes can be estimated from the splitting of  $n_{eff}$  of the originally degenerate modes. This splitting gives us the beat length between those near-degenerate supermodes, i.e. the propagation length required to accumulate a  $2\pi$  phase difference between two modes, and transfer power from one part of the waveguide to another and back again. Hence, a particular near field pattern (e.g. light into one individual core) will remain unchanged over lengths considerably shorter than the beat length. We calculated the beat length between the lowest and highest order near-degenerate supermodes at the wavelength of  $1.55 \mu\text{m}$  as shown in Fig. 4 (red line, secondary axis). A near-diffraction limited waveguide propagates light in the fundamental mode i.e. a near-diffraction limited Gaussian beam. By this definition our photonic lantern transitions would be near-diffraction limited even when small coupling between the cores occurs due to a small splitting of the  $n_{eff}$  of the near-degenerate supermodes. For these photonic lanterns to operate in a similar fashion to those experimentally demonstrated previously in [4,5], the coupling between the cores should be negligible for the length of interest. A core separation in the range of 30 to 40  $\mu\text{m}$  will give a beat length of around 90 to 10,000 m, which should be enough for any practical application of these devices.

The restriction on the degenerate single-mode operation at the large OD end does not offer any intuitive information about the modal evolution along the photonic lantern transition itself. Bringing the cores closer together would perturb the modes and cause a splitting in the  $n_{eff}$  that is larger and with an earlier onset than observed in Fig. 3, in which the core separation was 80  $\mu\text{m}$ . In order to study the interaction between cores and cladding modes along the transition we calculated the modal evolution for three different multicore photonic lanterns with core separations of 20, 40 and 60  $\mu\text{m}$  and the same parameters used previously. The results shown in Fig. 5, give clear evidence of the importance of the core separation on the photonic lantern modal evolution behaviour. A larger and earlier onset of the  $n_{eff}$  splitting of the 14 originally degenerate vector modes into the five scalar supermodes occurs. At the large



OD end of the transition with large core  $V_p$  parameters the effect of the splitting is not as relevant. As the transition evolves and the cores decrease in size and  $V_p$ , the closer proximity of the cores becomes more dominant in the modal behaviour of the transition leading to a larger perturbation on the guiding properties of the individual cores. This larger perturbation is represented by a broader splitting of the  $n_{eff}$  of the core modes which leads to an inevitable overlap with the cladding modes of the multimode structure as clearly shown in Fig. 5.

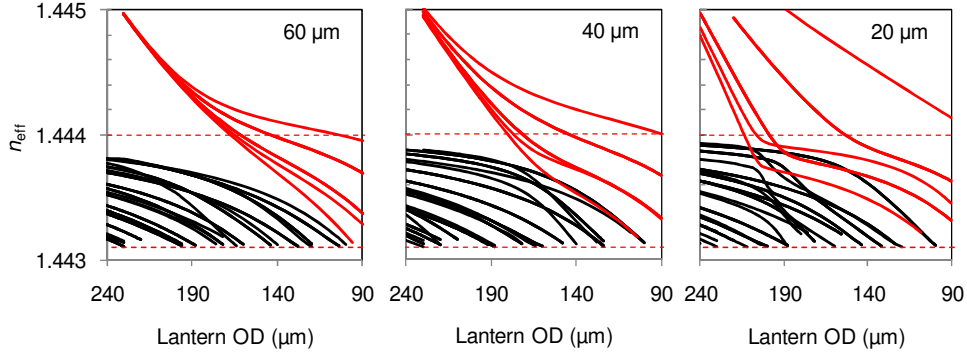


Fig. 5. The evolution of modes throughout the end of the tapered transition of the photonic lantern for different core separation. The cores have the following properties:  $n_{co} = 1.45397$ ;  $n_{cl} = 1.444$ ;  $d = 6.5 \mu\text{m}$ ; core separation of (Left)  $60 \mu\text{m}$ ; (centre)  $40 \mu\text{m}$ ; and (right)  $20 \mu\text{m}$ .

A core separation of 60 to  $50 \mu\text{m}$ , as in Fig. 5, would still be acceptable for a reversible low-loss photonic lantern as the core and cladding modes are well separated, as in the original design. At  $40 \mu\text{m}$  separation, the highest order core mode intersects with and then begins to overlap in  $n_{eff}$  with the lowest order cladding mode and subsequently with an additional cladding mode. In the forward propagation direction, from the single-mode fibres to the multimode core, the slightest perturbation or deviation from adiabaticity will present an opportunity of coupling between these modes. This will not present a problem in the forward propagation, as these three modes appear to be cut-off at the same OD. If the lantern is terminated at a sufficiently large OD ( $\sim 110 \mu\text{m}$ ), then all three modes will be guided and any coupling between them will not result in loss. In the reverse direction however, the proximity of the three modes in  $n_{eff}$  does pose a problem as light will be launched into and/or couple between all three. The fraction launched or coupled into the cladding modes will evolve accordingly, resulting in loss in the device.

In the  $20 \mu\text{m}$  core separation case the modal evolution becomes more complicated. The splitting between the core modes becomes significant very early in the transition pushing the core modes into lower  $n_{eff}$ . Three of the five scalar core modes interact with cladding modes of the same symmetry and display avoided crossing at OD  $\sim 190 \mu\text{m}$  (this is indicated by a sudden change in the gradient of the  $n_{eff}$  curve in Fig. 5, right). In addition, the core and cladding modes intersect many times for OD  $< 210 \mu\text{m}$ . All these provide opportunities for loss through coupling to cladding modes. In the single-mode to multimode direction, the avoided crossings and intersections provide an opportunity for the light to couple to cladding modes which are cut off at larger OD. In the reverse direction, the overlap between the highest order core mode and lowest order cladding mode (as in the case of  $40 \mu\text{m}$  separation) means that light cannot be coupled exclusively into the core modes to begin with, thus presenting a further loss mechanism in addition to potential coupling between the core and cladding modes.

These results show how critical the design of a multicore photonic lantern is and how strongly it depends on the core separation. At the  $20 \mu\text{m}$  core separation, the splitting is as low as  $\Delta n_{eff} \sim 10^{-6}$  between the lowest and the highest  $n_{eff}$  of the near-degenerate core modes at the large OD end of the photonic lantern which seems negligible, however, it makes a significant

contribution to the mode evolution in the transition, leading to a high-loss device. For a perfect adiabatic transition with no perturbations, the intersections of the modes in  $n_{eff}$  and the avoided crossings should not result in any coupling, yet even in this ideal case, the degeneracy of the highest order cladding mode and lowest order core mode would be a problem in the reverse propagation (from the multimode core to the single-mode cores). The presence of the avoided crossings and intersections does place very strict tolerances on the quality of the transition, so it is best to avoid their occurrence altogether and design the lanterns with sufficiently separated cores so as to produce a more robust device.

## 5. Conclusion

The modal evolution and a study of the core design for the photonic lantern devices have been presented. We have shown that a low-loss multimode waveguide coupling to an array of degenerate single-mode (i.e. near-diffraction limited) fibres/cores is indeed possible. We have presented the ideal parameters for these waveguides to work, based on the parameters used in [4], the core separation at the large OD end must be at least  $60\ \mu\text{m}$  to ensure low loss propagation in both directions. We have also introduced an intuitive QM analogy of the modal evolution along photonic lanterns based on the Kronig-Penney model of periodic quantum wells, thus giving an analogy between fibre optic cores and quantum wells.

One aspect not explicitly addressed was the operation of the photonic lantern at different wavelengths. Ignoring chromatic dispersion, information about different wavelengths is already presented in the modelling in Figs. 3 and 5 of the tapered transition, as scaling the waveguide down to a smaller OD is equivalent to increasing the wavelength by the same factor. Thus the modes at  $1.55\ \mu\text{m}$  and an OD of  $170\ \mu\text{m}$  are identical to those at  $1\ \mu\text{m}$  and an OD of  $110\ \mu\text{m}$ , and similarly  $1.55\ \mu\text{m}/\text{OD of } 95\ \mu\text{m}$  is equivalent to  $1.8\ \mu\text{m}/\text{OD of } 110\ \mu\text{m}$ .

This work has focused on the modal evolution at different points of the transition; hence no attempt to study the adiabaticity criteria for the propagating modes for the tapered regions themselves were made. Further studies need to be done in order to fully characterize these complex devices, taking into account the adiabaticity and also a wider range of core geometries and other waveguide parameters than addressed here.

## Acknowledgement

Joss Bland-Hawthorn is supported by a federation Fellowship from the Australian Research Council. Authors would also like to thank Boris Kuhlmeiy and Andrew Docherty for useful discussions about the use of the modelling software.